Lab on a Chip

Accepted Manuscript

ROYAL SOCIETY OF CHEMISTRY

www.rsc.org/loc

Lab on a Chip

RSCPublishing

PAPER

Microfluidic static droplet array for analyzing microbial communication on a population gradient†

Cite this: DOI: 10.1039/x0xx00000x

Heon-Ho Jeong,[+,a] Si Hyung Jin,[+,a] Byung Jin Lee,[a] Taesung Kim,[b] and Chang-Soo Lee*[a]

Quorum sensing (QS) is a type of cell-cell communication using signal molecules that are released and detected by cells, which respond to changes in their population density. A few studies explain that QS may operate in a density-dependent manner; however, due to experimental challenges, this fundamental hypothesis has never been investigated. Here, we present a microfluidic static droplet array (SDA) that combines a droplet generator with hydrodynamic traps to independently generate a bacterial population gradient into a parallel series of droplets under complete chemical and physical isolation. The SDA independently manipulates both a chemical concentration gradient and bacterial population density. In addition, the bacterial population gradient in the SDA can be tuned by a simple change in the number of sample plug loading. Finally, the method allows the direct analysis of complicated biological events in an addressable droplet to enable the characterization of bacterial communication in response to the ratio of two microbial populations, including two genetically engineered QS circuits, such as the signal sender for arcyl-homoserine lactone (AHL) production and the signal receiver bacteria for green fluorescence protein (GFP) expression induced by AHL. For the first time, we found that the population ratio of the signal sender and receiver indicates a significant and potentially interesting partnership between microbial communities. Therefore, we envision that this simple SDA could be a useful platform in various research fields, including analytical chemistry, combinatorial chemistry, synthetic biology, microbiology, and molecular biology.

Received 00th January 2012,
Accepted 00th January 2012

DOI: 10.1039/x0xx00000x

www.rsc.org/

Introduction

Cell-cell communication is a fundamental activity performed by most cells. Bacteria often use cell-cell communication to assess their population density in a process called quorum sensing (QS).[1-3] From single species to multispecies, they can secrete and sense the same signal molecules that accumulate in the growth medium as cells grow to a high population density. The QS allows populations of cells to control a variety of traits, including virulence factors, nutrient scavenging molecules, and growth compounds.[4-8] For instance, QS-regulated antibiotics are produced to kill or impair emulative species that protect the viability and function of pathogenic bacteria.[9] Certain communities of soil microorganisms have beneficial interactions that are coordinated among multiple species under nutrient-poor conditions.[10] Although the mechanisms underlying production, uptake, and response to these signal molecules are understood, relatively little is known about how QS operation corresponds to the density difference between signal senders and receivers.[11-14] Because understanding these positive or negative interactions in microbial communities is an important scientific issue in biology, an effective analytical tool is essential to evaluate cell-cell interactions and to monitor the response of the compartmentalized cell environment to different population ratios of the signal sender and receiver.

The demand for a biological screening assay motivates the development of microfluidic devices as an emerging powerful, inexpensive alternative to conventional multi-well plate systems, providing a significant benefit by compartmentalizing distinct reactions in very small volumes with various combinatorial compositions.[15-19] Currently, the most promising microfluidic methods to control reagent concentration, rapid mixing of fluids, and dimensional scaling benefits are droplet-based array systems.[20-22] These systems' capabilities have made them an attractive platform for biological assays and screening. However, there are few reports on performing cell-cell interaction assays with controlled population cell density pairs due to technical challenges. Currently, there are two approaches to producing concentration gradients, the mobile droplet array (MDA) and the static droplet array (SDA).[23-32] In the case of the MDA, the composition of the droplet is manipulated by adding and diluting the reagent using coalescing droplets under an external force, such as an electrical field or fluid pressure via pico-injector.[33-34] However, the MDA method is limited in its

ability to produce concentration gradients in droplets that contain living cells. Moreover, it is hard to index a droplet based on position and perform a long-term monitoring assay. The SDA is a format of miniature multi-well plates with picoliter scale droplets stored at predefined locations.[24-30] It provides the ability to perform simultaneous reactions or assays in droplets with a wide range of concentrations and time-scales. We can easily index or code each individual droplet's position. Although pioneering works show promising results for the concentration gradients of chemicals, particle, and red blood cells using fluid mixing and sedimentation effect in the SDA, they are still limited in generating droplet arrays containing single bacteria or two different species. [24-30, 35-36] Therefore, there is a great needs for simple SDA format to control bacteria concentration in a tunable manner from droplet to droplet and to add a second type of bacteria to a well-defined parallel droplet position.

Here, we present a microfluidic SDA that combines a droplet generator with a droplet array to independently generate a bacterial population gradient into a parallel series of droplets under complete chemical and physical isolation. The basic principle of generating the gradient is that a long moving plug containing one bacterial species sequentially exchanges and extracts from the on-array droplet containing another bacterial species, allowing partial mixing of the two species inside the long plug. Thus, the number of bacteria in the droplet array is tunable through the sequential merging and mixing of the moving plug with the trapped droplets. We successfully demonstrate the function of the SDA with a reverse gradient of two bacterial populations and investigate the effect of population ratio on cell-cell interactions between the signal sender (production of signal molecules) and receiver bacteria (signal molecule receiver). This study reveals critical roles of the population ratios between sender and receiver bacteria in bacterial QS.

Experimental

Escherichia coli strains and culture

As listed in Table S1, for the bacterial concentration gradient and communication experiments, four different plasmids were transformed into competent *E. coli* MG1655. All of the plasmids conferred ampicillin resistance. First, two transformed mutants of *E. coli* MG1655 constitutively express either green fluorescent protein (GFP) or red fluorescent protein (RFP) (JBEI, USA). Second, two plasmids were transferred from the Registry of Standard Biological Parts (www.partsregistry.org) and transformed into competent *E. coli* MG1655.[37-38] In this work, we refer to plasmid pTKU1-11S as the "sender" because this plasmid constitutively produces LuxI, which is converted into acyl-homoserine lactones (AHLs); its MW is 213.23 as purchased from Sigma–Aldrich, and the diffusion coefficient is assumed to be $D_{AHL} = 0.8 \times 10^{-9}$ m^2/s. Similarly, we refer to plasmid pTKU1-12R as the "receiver" because the AHLs produced by the "sender" cells (SCs) diffuse to the neighboring "receiver" cells (RCs). In other words, the RCs are activated to express GFP by the AHL produced from SCs.

To culture these bacteria, each *E. coli* culture was grown overnight on M9 solid agar medium plates with 100 μg/ml ampicillin at 32 °C. A single colony was used to inoculate 5 ml of M9 media with both antibiotic (100 μg/ml ampicillin) and 10 mg/ml (1%) glucose. The cultures were then grown overnight (16 h) with vigorous aeration (200 rpm in a rotary shaker), resulting in an OD_{600} (optical density at 600 nm) of 3.0. The bacteria were centrifuged at 5000 rpm (Eppendorf 5424, Hamburg, Germany) for 5 min, and the pellets were resuspended with fresh M9 media to yield bacterial suspensions with the desired bacterial densities.

Microfluidic device fabrication

The microfluidic device was fabricated by soft lithography to integrate microvalves using polydimethylsiloxane (PDMS) (Sylgard 184, Dow Corning, USA). Two different master molds were fabricated by photolithography to create the fluidic and microvalve channels. The fluidic layer master was prepared on a silicon wafer by spinning SU-8 3025 negative photoresist (Microchem Corp, Newton, MA) at a thickness of 20 μm and patterned by photolithography. The valve layer master was patterned in a same way and the thickness was 20 μm. The PDMS prepolymer and its curing agent (10 : 1 ratio) were poured onto the master mold for the fluidic layer, cured in a 65 ºC oven for 60 min, and peeled off from the master mold; injection holes were then punched into the fluidic layer. The bottom pneumatic microvalve layer was formed on the master mold by spin-coating the PDMS mixture (20 : 1 ratio of prepolymer and curing agent) at 3000 rpm for 1 min and curing at 65 ºC for 45 min. Then, the fluidic layer was aligned over the microvalve layer and cured in a 65 ºC oven for overnight. The PDMS chip with the fluidic and microvalve layers was peeled off from the master mold, and holes were introduced to connect the inlet ports to the microvalve channels. Finally, the PDMS chip was bonded to a glass slide by plasma treatment for 1 min and then kept in a 65 ºC oven for 2 hours to improve the bonding strength.

Device operation

Importantly, simple soaking of the SDA into sterilized water for 3 days can dramatically reduce droplet evaporation. And then, the SDA is soaked into sterilized water while performing bacterial communication experiment. The microfluidic device was operated using homemade solenoid valve manifolds and a controller (Stanford Microfluidics Foundry, USA). A USB controller board mounted in the computer controlled the switching of each channel of the manifolds. The individual microvalves were operated using a custom-built LabVIEW (National Instruments Co., Austin, TX) program. Nitrogen gas was used to inject the reagents into the microchannels and microvalves. Prior to starting the experiment, we filled the microvalve with sterilized water. FC-40 oil with 20% 1H,1H,2H,2H-perfluorooctanol as the continuous phase and aqueous solutions for the dispersed phase were injected into a microchannel.

Generation of bacterial concentration gradient

RCs and SCs (OD_{600} = 3.0) suspended in M9 media were introduced into each inlet port with closed microvalves to prevent cross-contamination. In the state in which the microvalves of the array chamber (0.3 MPa) were closed, a long droplet plug (7 nL) containing RCs was generated to trap droplets in the array chamber. Then, the droplet plug of SCs (2 nL) was generated to merge and mix with the SDA containing RCs. The bacteria were monitored using a fluorescence microscope (TE-2000, Nikon, Japan) equipped with a high-resolution CCD camera (Coolsnap, Roper Science, USA).

ImagePro (Media Cybernetics, MD, USA) software was used for the fluorescence analysis of each image.

Bacterial growth curves and glucose assay

All growth curves and a glucose assay were simultaneously performed using SCs, RCs, and RCs in the presence of 10 μM AHL, as appropriate. During cultivation at an initial OD_{600} = 0.5, the culture medium was collected to measure the growth rate and glucose concentrations using a glucose assay kit (Sigma) and a UV spectrometer (UV-VIS 300, Thermo Scientific, USA).[39-40]

Results and discussion

Principle of droplet trapping in a microfluidic device

A schematic diagram and images of the SDA integrated with microvalves are shown in Fig. 1. The SDA fabricated with PDMS by multilayer soft-lithography consists of two functional parts: a plug generation part and a droplet array part. In the plug generation part, we design T-junction structures to produce multiple plugs and integrate with a pneumatic microvalve in the aqueous flow channel to control the flow of the aqueous phase on demand in real time. When the microvalve is switched off, the aqueous solution flows out of the T-junction and is surrounded by immiscible oil. When the microvalve is switched on, the flow of the aqueous solution is cut off, and a plug forms instantly. By alternately switching on and off, plugs are reliably produced, and the size of the plug can be tuned precisely by the duration of the off-status of the microvalve. Different samples with a desired plug composition can be separated without contamination of each droplet in a single device (Fig. 1A). The plug generated from the plug generation part is transported into the droplet array part. The droplet array part contains a microfluidic network with a repeated sequence bypass loop that has lower hydrodynamic resistance and a hydrodynamic trap array integrated with trap valves (Fig. 1B). The detailed geometry and the cross section of the hydrodynamic trap are shown in the supplementary information (Fig. S1). Briefly, the hydrodynamic trap with its narrow entrance (40 μm) and circular chamber structure (100 μm diameter) provides stable hydrodynamic trapping of the droplets. The trap valve is also integrated at the exit position of the trap and controls the flow resistance (R_1), which manipulates the direction of the fluid flux toward the trap or bypass loop (Fig. S1). Although we adopt the basic principle of formation of the droplet array by the previously reported method,[25, 30, 41] there is still great need for the capture of a flexible and elastic droplet in a highly controllable manner. Here, we construct a novel SDA by integrating a microvalve into the trap and designing the trap with geometrical constriction.

When sample plug generated from plug generation part moves into droplet array part, the plug is sequentially trapped and formed droplet array in hydrodynamic traps. The basic principle of forming SDA follows hydrodynamic trapping previously reported by pioneering groups.[25, 30, 41-43] As shown in Fig. 1B, a SDA consists of a series of bypass loop channels superimposed onto a straight hydrodynamic trap. The SDA has two volumetric flows such as individual trap (Q1) and bypass loop channel (Q2); there is hydrodynamic competition between individual trap (Q_1) and bypass loop channel (Q_2). Hydrodynamic trapping utilizes the hydrodynamic competition of those two volumetric flow rates at the hydrodynamic trap. When an individual trap is empty, Q_1/Q_2 is larger than 1 and the head part of plug is introduced into individual trap because the individual trap has a lower flow resistance than that of the bypass loop channel. As a result, the plug is not able to enter bypass loop channel and fills the individual trap because bypass loop channel act as a capillary valve. Reversely, after filling the individual trap, Q_1 is decreased and then Q_1/Q_2 is decreased below 1. Thus, relatively high volumetric flow rate of bypass loop channel (Q_2) results in moving of plug along bypass loop channel and flows into the next hydrodynamic trap.

The strong advantage of SDA device integrated with valves is

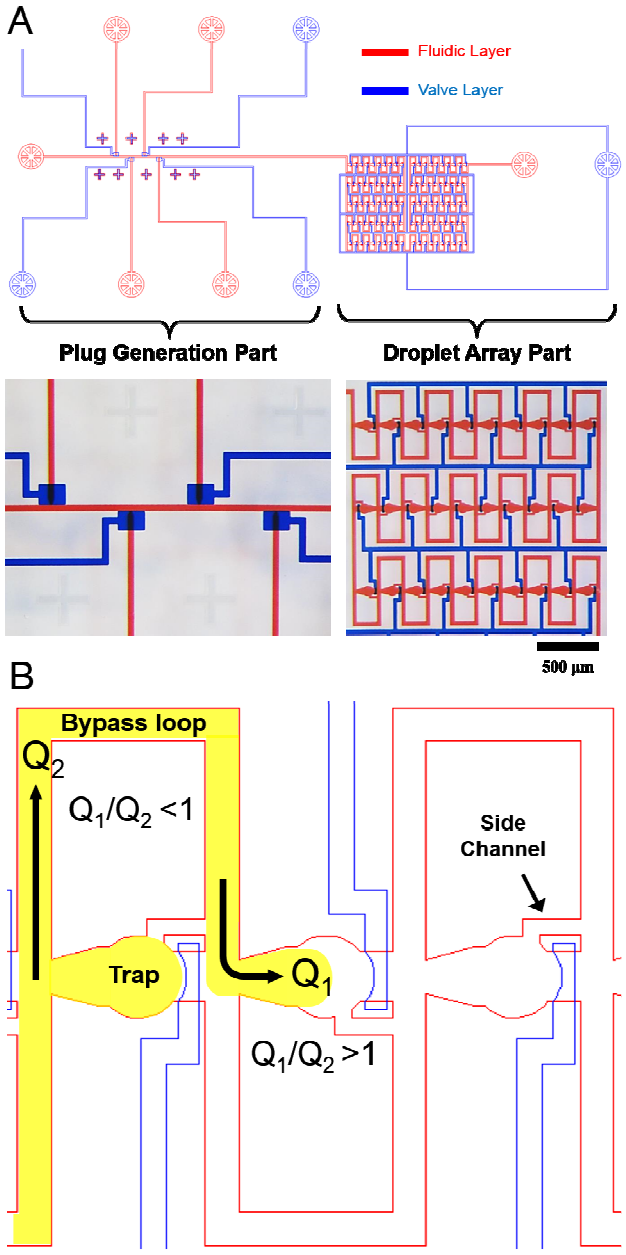

Fig. 1 Design of SDA integrated with microvalves and hydrodynamic trap array. (A) Schematic design and optical images for plug generation and droplet array parts. The red and blue lines indicate microfluid channels and microvalves, respectively. (B) Detailed diagram of microfluidic network and hydrodynamic trap. There are two main flows (Q_1: trapping flow and Q_2: bypassing flow). The microvalve elegantly provides hydrodynamic resistance in the trap.

precisely to control hydrodynamic flow of Q_1/Q_2 by simple operation of trap valve. The trap valve can be pneumatically actuated to open or close microfluidic channel in individual hydrodynamic trap. When the trap valve is given a command to open at a certain point (so we called "off"), the horizontally laid microchannels in the hydrodynamic trap are opened; Q_1/Q_2 is equals to 20.5 based on mathematical calculation, which means that Q_1 is extremely higher than Q_2 (see Supplementary Information). Thus, the sample plug is flowing through individual trap without hydrodynamic trapping. When trap valve is switched on, it partially closes horizontal fluidic microchannel in hydrodynamic trap. Thus, small cavities are generated at the edge of rectangular microchannel (Fig. S1B). Those small cavities and side channel provide an appropriate fluidic flow of Q_1 to trap sample plug; Q_1/Q_2 is equal to about 3.19. Therefore, in this regime of Q_1/Q_2, we can successfully perform hydrodynamic trapping of sample plug into empty trap and generate well-defined droplet array in series hydrodynamic traps without any releasing and splitting problem because three residual flows exist in individual trap and the increase in volumetric flow of the bypass loop (Q_2) allows a portion of the sample plug to fill the trap.

Generation of gradient droplet array and release

The basic principle of generating a droplet array generates the SDA in a simple manner. The representative time-lapse images show the continuous sequence of the generation of an SDA (Fig. 2). When we turn the microvalve on, a sample plug moves into the hydrodynamic trap, and the head of the plug fills the entrance of the trap as expected (Fig. 2A). The capillary pressure at the geometrical constriction of the trap limits further movement. As the plug continues to traverse other bypass loops, this plug sequentially fills each trap and then moves into the bypass loop channel to fill next trap due to the difference in flow resistance (Fig. 2). In accordance with this basic principle, we can produce an SDA of uniform composition and size (180 ± 2.23 pL). Then, we introduce a second plug into the SDA, and the entire process is shown in Fig. 2B. While the head of the second plug goes forward into the array, the thin film of oil between the stationary droplet and the moving plug ruptures, allowing exchange of materials at the entrance of the trap (Fig. 2B, Fig. S2). Fig. S2 shows a detailed sequence of images of the exchange dynamics. The exchange of materials occurs at every trap as the secondary plug travels through the whole trap, which is the main driving force to produce the concentration gradient series in the array (Fig. 2B). The first droplet at the first trap inter-mixes with the second plug, and the successive droplets are diluted with increasing amounts of materials from

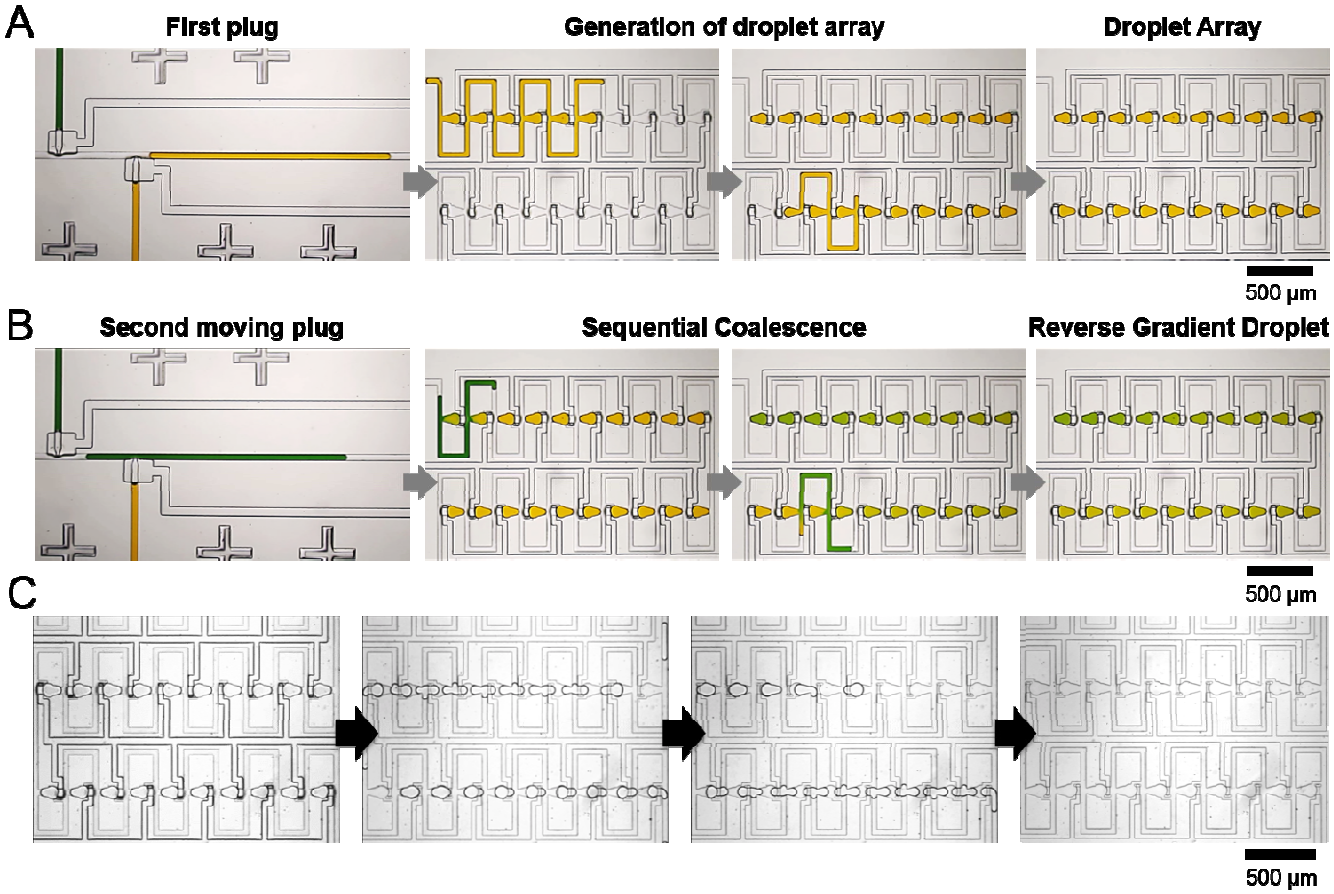

Fig. 2 Principle of generation of chemical concentration in an SDA. (A) Sequential images showing the consecutive process of droplet array formation. The plug generation (left), generation of droplet array (middle), and final droplet array (right). (B) Optical images of sequential dilution by the secondary moving plug. We can obtain two reverse gradients of chemical concentration. (C) Release of all droplets from the SDA. The SDA can be reused by a simple switch-off operation until the adsorption of materials occurs. In our experiments, there was no significant adsorption for 30 uses.

the first one. Finally, we generate two types of concentration gradients, increasing and decreasing gradients in the first (yellow) and second (green) droplet arrays, respectively. The approach clearly indicates that simply changing the composition of the first and second plug in the plug generator flexibly manipulates the increasing or decreasing concentration of the soluble materials from droplet to droplet in the array. These results confirm the generation of a chemical in an SDA via simple production, transportation, storage, and mixing of droplets. Furthermore, the advantage of this approach is that simply switching off the microvalves easily releases all droplets from the SDA (Fig. 2D and Movie S1). The released droplets move downstream along the array microchannels. After releasing all droplets from the SDA, we can reuse the SDA by reloading the sample plugs.

Characterization of bacterial population gradient

Most biological applications require complex, non-soluble materials, such as cells, rather than soluble materials. In particular, cell-based screening handles a population of cells along with numerous drugs at various concentrations.[44-45] Several studies report that the population gradient quantitatively or qualitatively regulates cell-cell interactions and determines many biological or physical connections that a single cell is able to establish with surrounding cells, which in turn regulate cell behavior by influencing the intracellular signal transduction pathway.[46-47] In addition, spatial variations in cell density may lead to the development of another biochemical gradient, as a result of which cell migration, proliferation, and differentiation can be affected.[11, 48-50] The ability to generate a controllable population gradient is critical to the recreation of functionality for many types of biological events.[51-52] In a sense, the ability to generate a population gradient is essential for the fundamental study of cell-cell interaction.[53-55]

We want to expand our method to create a bacterial population gradient for cell-based assays (Fig. 3A). To demonstrate this feasibility, we sequentially loaded two plugs, a buffer plug followed by a bacterial plug. To create a clear visual image and precisely quantify the number of bacteria in each droplet, we used bacteria expressing green fluorescence protein (GFP) as a proof of concept. As expected, bacteria in the second plug were transported to the preloaded phosphate buffer array, and a decreasing bacterial population gradient was obtained in the SDA (Fig. 3A). The time-lapse fluorescence images clearly indicate the serial dilution of bacteria in the SDA. The initial bacteria plug with a high density (OD_{600} = 3.0) was sequentially transported to each trap to achieve a decreasing concentration gradient; thus, the first droplet in the SDA contains a high concentration of bacteria, and the moving bacteria plug is continuously diluted as it sequentially merges with pre-trapped droplets while traversing the bypass loop network. The dynamics of bacterial exchange between immobilized droplet and moving plug is shown in Fig. S3. When moving plug contacts with immobilized droplet, transportation of bacteria from moving plug to trapped droplet is triggered from rupturing and coalescence of oil-water interface, which results in rapidly forming a convective flow from plug into droplet. Thus, bacteria in moving plug are transported along with trap wall. Bacteria at middle region of moving plug cannot penetrate into immobilized droplet while passing through the trap. When moving plug's tail arrives at trap, strong convective flow occurs within immobilized droplet because of biased shear force of plug streaming driven by gradual increase of volumetric flow rate toward bypass loop channel (Q_2). After that, the plug and immobilized droplet are segregated. We consider that the

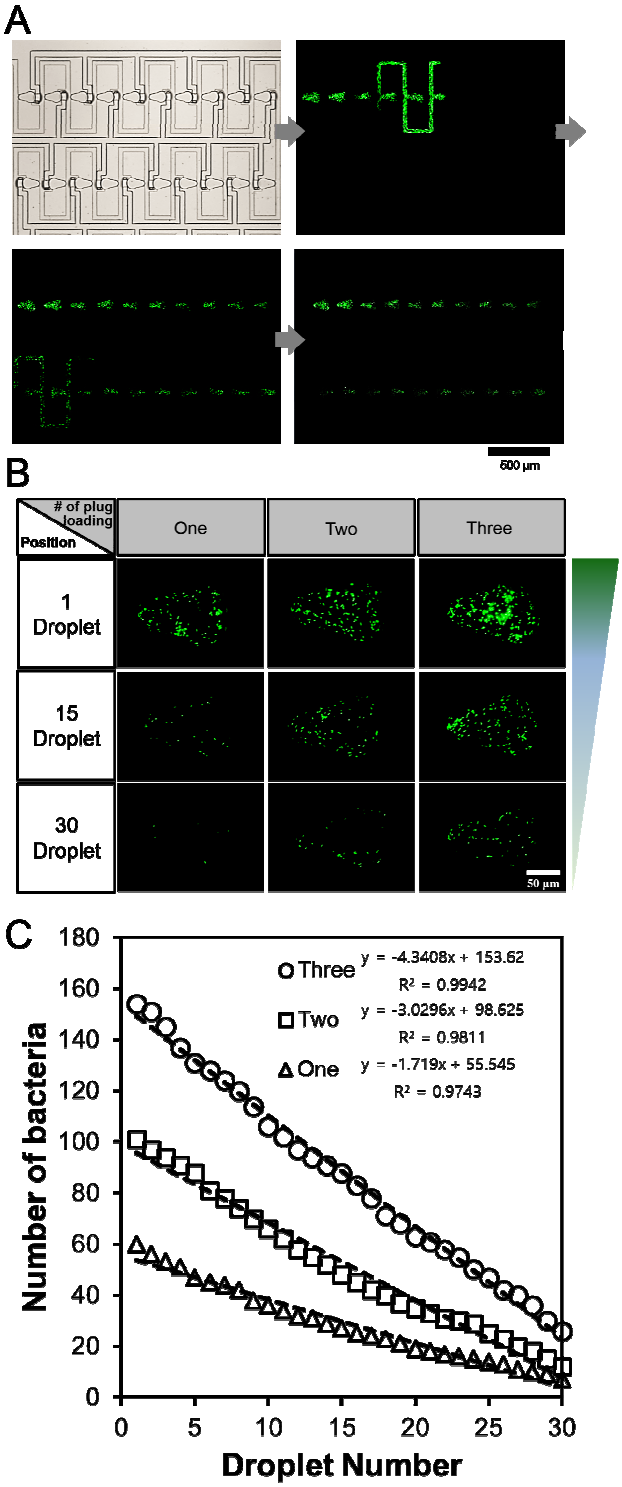

Fig. 3 Gradient of bacterial population in the SDA. (A) Time-lapse fluorescence images of the bacteria dilution procedure. (B) Fluorescence images for GFP-expressing bacteria in each droplet with increasing loading time of the moving plug. (C) Quantitative linearity of the population gradient of bacteria. Dashed lines indicate linear regression. All lines show high fidelity in controlling the bacterial population.

convective flow within droplet is attributed from viscous-drag force from the shearing of oil fluid toward bypass loop channel (Q_2). To induce high drag force in droplet and increase average flow rate at oil-water interface, we have designed tear shaped hydrodynamic trap combined with three residual flows (Fig. 1 and Fig. S1). Based on the principle, we finally obtain strong convective flow within the immobilized droplet.

We investigated whether the SDA is able to make a serial dilution of bacteria soup and control the slope of a concentration gradient in consecutive droplets because most biological screening assays address complex insoluble materials, such as bacteria (Fig. 3). To simply evaluate its capacity for the serial dilution of bacteria, we used bacteria expressing GFP because the number of bacteria is easily measured by simply counting the number of fluorescence spots using fluorescence microscopy. According to previously established procedures, we successfully produced a droplet array containing thirty sequential buffer droplets. Then, a bacterial plug sequentially traversed and interacted with each droplet. As expected, a population gradient of bacteria in the SDA was successfully developed (Fig. 3B). The fluorescence images of the 1st, 15th, and 30th droplets clearly showed the gradual decrease in the number of bacteria in each droplet (Fig. 3B). Increasing the loading time increases the bacterial concentration at the same droplet position and the steepness of the bacterial population gradient (Fig. 3C). Because the high-population bacterial plug is preferentially merged with upstream droplets and is continuously diluted, the upstream droplets exhibit a huge increase in bacterial population, while the downstream droplets exhibit a small increase (Fig. 3C). All linear regressions provide a close fit to the experimental data, indicating that the bacteria population is linearly controlled by the position of the droplet. The linear relationship between the number of loading times of the moving plug and the bacteria population supports the capability of the SDA. These results confirm that the slope of the bacterial population gradient can also be simply adjusted by repeating the loading of the bacteria plug. Importantly, we can readily achieve an elaborate dilution of bacteria with small changes between adjacent droplets, allowing precise understanding of the behaviors involved in cell-cell interactions, such as whether the quantitative data follow a linear or non-linear relationship. Thus, the experimental flexibility of our device could be very practical for interrogating the alterations of living cell behaviors, such as antibiotic susceptibility, chemotaxis, and QS, in response to external stimuli.

The advancements and novelty of this work are as follows: 1. The microfluidic SDA integrated with a microvalve system consists of both plug generation part and droplet array part. We can perfectly solve cross-contamination of reagents from the

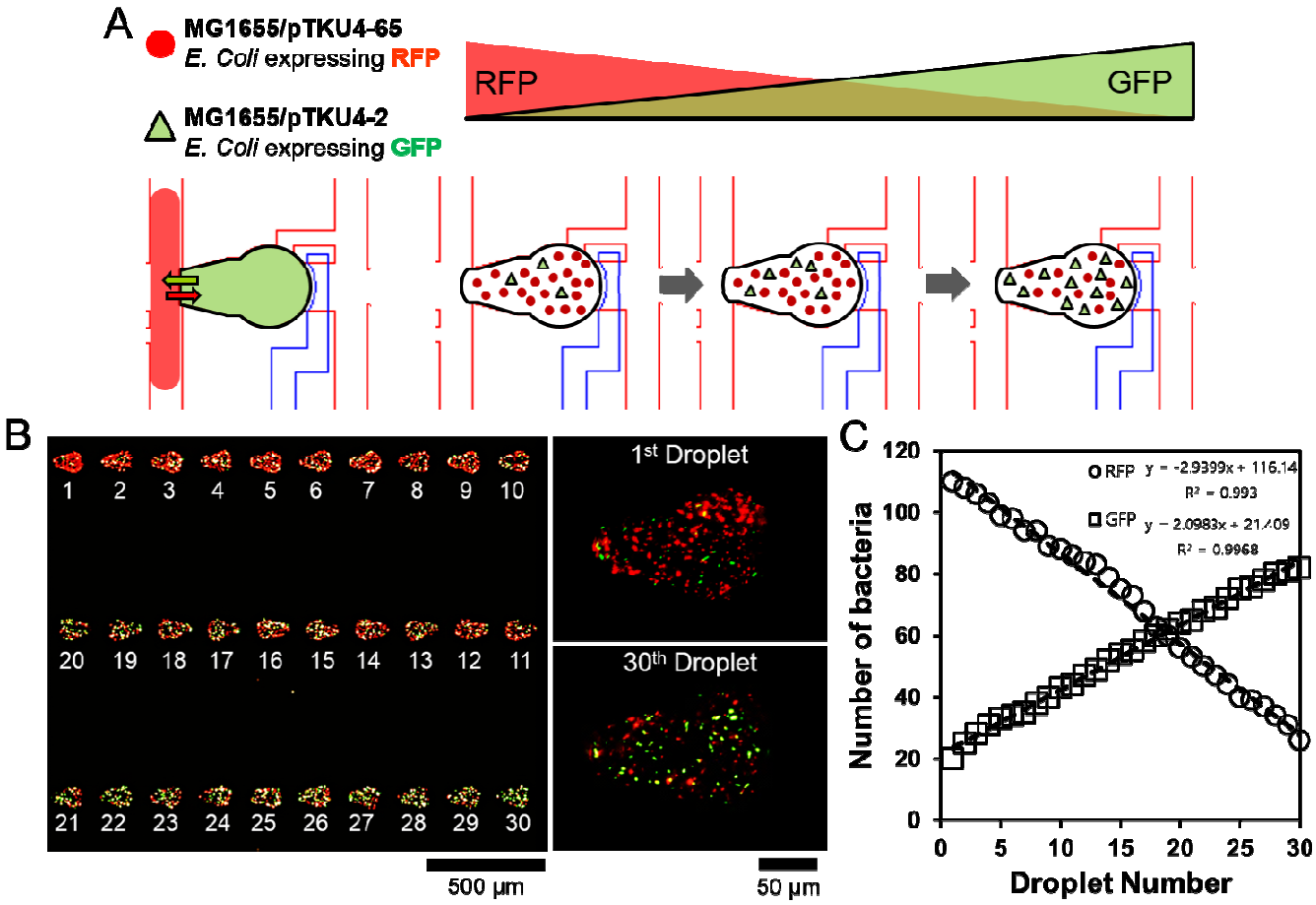

Fig. 4 Generation of a reverse gradient of two bacteria population. (A) Schematic principle for generating a reverse gradient in an SDA. (B) Fluorescence images of GFP- and RFP-expressing bacteria in an SDA. The enlarged images at both the first and last droplets indicate distinct changes in the two bacteria populations. (C) Linearity of the reverse gradient of the bacteria population. Generation of reverse gradient is performed with 2 nL plug of bacteria solution at flow rate of 2.1 mm/s for three times.

initial droplet generation step using separate reagent channels and microvalves. In addition, the SDA integrated with microvalves can freely control the volume and composition of droplet regardless of spatio-temporal restriction. 2. In contrast to conventional droplet arrays, this SDA can be perfectly reused for several times. This robust release system provides capability to perform high-throughput screening (HTS) in a re-usable single chip without contamination and destroying the SDA. 3. To our knowledge, it is first report to demonstrate a bacteria population gradient with single and two specices in droplet array format although several methods have previously shown concentration gradients of soluble materials, microparticles, and animal cells. The principle of concentration gradients of insoluble materials such as bacteria in the SDA follows simple hydrodynamic mechanisms of coalescence, mixing, and consecutive trapping and traversing. By adjusting number of loading of plug into the droplet array part, various gradient patterns can be easily produced in a controllable and reproducible fashion. In addition, reverse gradient of different cell types can also be produced on the same droplet array by taking advantage of sequential loading processes.

Reverse population gradient for cell-cell interactions

Furthermore, we extended our approach to produce a reverse population gradient of two bacteria using the ability to add and remove materials from trapped droplets, as multi-component droplet arrays are an essential characteristic of screening assays. Figure 4 illustrates that our method is capable of creating a reverse population gradient of two bacteria. First, we sequentially loaded RFP-expressing bacteria and GFP-expressing bacteria plugs because the basic principle of a population gradient is driven by the exchange of two types of bacteria between the moving plug and trapped droplets (Fig. 4A). In accordance with previously established protocol, plugs containing GFP-expressing bacteria are trapped into consecutive hydrodynamic traps, and then a moving plug containing RFP-expressing bacteria transverses along the microfluidic network. As expected, RFP-expressing bacteria in the moving plug are sequentially transferred to the trapped droplets, and GFP-expressing bacteria in the trapped droplets are also transferred into the moving droplet plug. Finally, we generated a reverse gradient of two bacteria populations (Fig. 4B). In the enlarged images of single droplets (first and thirtieth droplets), the first droplet shows a higher population of RFP-expressing bacteria, while the last droplet has a higher population of GFP-expressing bacteria. This simple regression also serves to underline the fact that the SDA can produce a highly desired gradient in two bacteria populations with high linearity ($R^2 > 0.99$), allowing the prediction of gradients without the use of GFP or RFP-expressing bacteria (Fig. 4C). Although the reverse gradient shows positive and negative linear slopes, the dilution rate is different between the two. This result indicates a discrepancy of dilution efficiencies between the moving plug and trapped droplets despite using two types of bacteria with the same population.

The possibility of population dependent cell-cell interaction

Next, we investigated cell-cell interactions in a population-dependent manner with a reverse population gradient. Two genetically engineered bacteria containing quorum-sensing circuits, a signal sender and receiver, were examined because QS is an important and complex mechanism of cell-cell communication that enables the coordination of group-based behavior based on population density. In general, the SCs can release signaling molecules including AHL, the most common class of autoinducer and product of the LuxI protein in Gram-negative bacteria.[14, 56] Signal molecules (AHL) freely diffuse into the extracellular environment. Upon reaching a threshold concentration of signal molecules in the extracellular environment, they diffuse into RCs and bind LuxR proteins to mediate transcriptional activation (Fig. S4). Although the mechanism of QS is well understood, and a dynamic control widely distributed in nature allows for whole-population coordination of gene expression, population-dependent behavior and nutrient-sensitive QS remain controversial and intriguing scientific issues.[57-58]

In particular, to our knowledge, there has been no experimental report on the effect of a population gradient on QS by precise control of the populations of signal sender and receiver bacteria. Thus, we expect that the utilization of SDA will pose a great challenge to current biological studies. First, a reverse population gradient was generated in SDA using two different plugs containing RCs or SCs. AHL produced from the SCs was transferred to RCs in confined droplet. Then, we measured the GFP expression level of RCs that responded to the concentration of AHL produced, as the analysis of fluorescence expressed from RCs clearly reflects communication between bacteria (Fig. 5). The SDA provided quantitative dynamic results estimated from each bacterium. QS enables coordination of the behavior of bacterial populations and is often controlled by extracellular environmental substances as nutrients or signal molecules from neighboring bacteria.[13, 14] As proof, an inducible gene expression system was chosen to investigate the effect of nutrient availability on QS. Under the nutrient-controlled condition (0.5X M9 medium), GFP expression from the RCs continuously increased in all droplets for 4 hours, and the RCs started to express GFP in response to AHL, while their individual expression levels varied (Fig. 5A). Interestingly, a high proportion of RCs resulted in an increase in the GFP signal from the 1st (RC: SC = 1 : 5.5) to the 30th droplet (RC: SC = 3.1 : 1). Namely, the quantification of the average fluorescence intensity of each droplet indicated a clear difference from the first to thirtieth droplet, meaning that there is population-dependent bacterial communication under the nutrient-limiting condition; the RCs express GFP at different levels in accordance with various population ratios between the RCs and SCs in 0.5X M9 medium (Fig. 5B and Fig. S5A). In addition, GFP expression is strongly associated with incubation time because AHL produced from SCs requires time to be synthesized (Fig. 5A). We also examined the quantitative change in GFP expression with various ratios of signal SCs to RCs in rich medium (1X M9 medium) (Fig. 5A and Fig. S5B). Noticeably, even the first droplet with a low proportion of RCs (RC: SC = 1 : 5.5) was able to achieve similar GFP expression to the 30th droplet. This result indicates that the population ratio does not influence bacterial communication in the nutrient-rich condition. This phenomenon confirms that the different population ratio does not influence the production of AHL, which is thus sufficient to perform QS in the rich media. To confirm the effect of nutrients on population-dependent cell-cell communication, we have examined the GFP expression of RCs as a function of nutrient concentration at a larger scale (500 ml flask culture) (Fig. S6). RCs were cultured at three nutrient concentrations (0.1X, 0.5X, and 1X M9 media) with the addition of 10 μM AHL. There was a dramatic decrease in GFP expression in RCs under severe starvation conditions

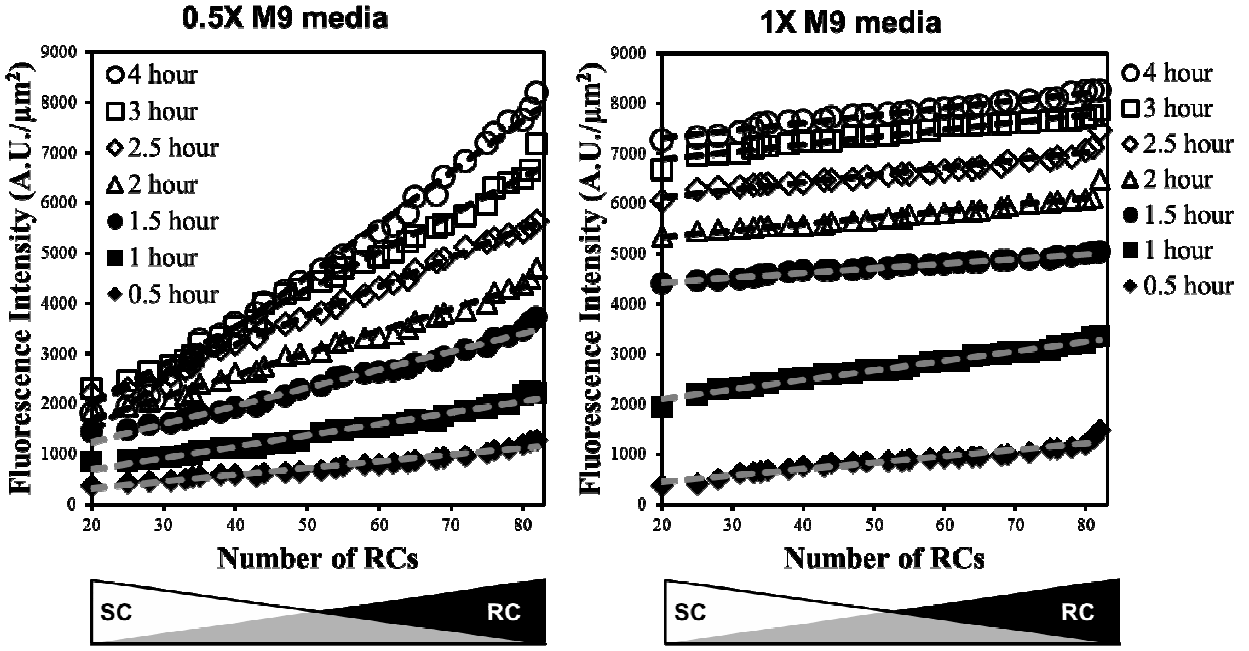

Fig. 5 Population-dependent cell-cell interaction. Quantitative data on GFP expression from RCs in relatively nutrient-poor (0.5X M9 media) and nutrient-rich conditions (1X M9 media).

(0.1X M9 media), although a sufficient concentration of AHL molecules was added in each case (Fig. S6). Thus, it is reasonable to assume that a decreasing nutrient supply down-regulates signal production activity; however, nutrient deficiency promotes signal production activity, at least within a certain range. All these results imply that the bacteria do not perform pure QS and integrate information about their individual demands into the communication signal. In the case of slight nutrient depletion, relatively starving bacteria may increase the production of signal molecules as an emergency call, demanding coordinated behavior. Consequently, these sequential processes reduce the number of SCs required to produce sufficient signal molecules to reach the induction threshold of GFP expression in RCs. If the population of RCs is very small, an emergency call will not have a strong effect, even if there is an increase in the production of signal molecules from a high population of SCs. The result obtained from SDA suggests that remarkable social behavior likely enables adaptive lifestyle optimization of coordinated cell-cell communication with respect to fitness and meaningful decisions in a specific environment. Additionally, we examined the consumption rate of glucose as a sole carbon source and the growth rate between RCs and SCs (Fig. S7). In the case of pure cultures of RCs and SCs, the rates of glucose consumption and growth are almost identical (Fig. S7A). The addition of AHL clearly decreases the rate of glucose consumption from 36 mg/*l*·hour to 25 mg/*l*·hour (Fig. S7A), while pure RCs and SCs exhibit no significant change. Interestingly, we found that the addition of signal molecules (AHL) to the culture medium for RCs significantly improved the growth yield compared to the yield in the absence of AHL (Fig. S7B). Commonly, QS involves the coordination of beneficial behaviors between bacteria through the production and secretion of diverse exo-products that result from the regulation of gene expression by the signal molecules.[14, 59] The beneficial behaviors in QS clearly occur in the transition state from the exponential to the stationary growth phase.[13] The improved growth yield implies that the RCs use AHL molecules not only for GFP expression but also to provide a beneficial effect to each other in large populations. In addition, the results of the glucose assay suggest that changes in gene expression via QS minimize the consumption rate of nutrients compared to the rate in normal conditions without signal molecules. In contrast, the presence of more RCs than SCs might lead to a stable QS system because of the slow nutrient consumption rate; furthermore, this population ratio might allow direct transportation of beneficial extracellular products to adjacent RCs because of the diminished interception of extracellular products, resulting in high GFP expression of RCs.

Our findings provide an example of SDA serving as a novel biological assay platform in a precise, quantitative manner. To our knowledge, although the presented results need further investigation in combination with molecular biology experiments, this method provides mechanistic insight into the nonlinear relation between nutrient conditions and QS via transferring signal molecules and assists in understanding the ecological purpose of signaling and coordinated social behavior.

Conclusion

In summary, we demonstrate a simple and robust microfluidic SDA for generating and controlling concentration gradients of various materials, including bacteria. In this SDA, the first droplet is positioned into an array format based on hydrodynamics, and a concentration gradient is created by mixing the two components between the moving plug and droplet, while the second moving plug transverses the bypass channel. By adjusting the initial concentration and multiple sequential loading of the moving plug, various gradient patterns can be easily produced in a controllable and reproducible fashion. Furthermore, a reverse gradient of different types of bacteria can also be generated on the same SDA by taking advantage of the simple individual loading process and

exchange of two bacterial populations. Here we find, for the first time, that QS may be influenced by the population ratio of the RCs and SCs. SDA is a useful biological assay platform to prove the existence of interesting sociobiological behaviors in population-dependent cell-cell interactions. Our finding suggests that the bacteria do not perform pure QS by integrating information about their individual demands into the communication signal and responding to it; instead, signal molecules rapidly saturate a certain threshold of signal receptors of RCs in the QS system. We envision that the controllable population gradient will enable a myriad of other biological applications, including enzyme or whole biochemical reactions, the optimization of biological assays, and biological screening.

Acknowledgements

This study was supported by a grant from the National Research Foundation of Korea (NRF) funded by the Korean government (MEST) (No. 2011-0017322).

Notes

[a] Department of Chemical Engineering, Chungnam National University, Yuseong-gu, Daejeon 305-764, Republic of Korea. E-mail: rhadum@cnu.ac.kr; Tel: +82 42 821 5896.

[b] School of Mechanical and Advanced Materials Engineering, Ulsan National Institute of Science and Technology, Republic of Korea.

† Electronic Supplementary Information (ESI) available: See DOI: 10.1039/b000000x/

[+] These authors contributed equally

References

1 Y. Afek, N. Alon, O. Barad, E. Hornstein, N. Barkai and Z. Bar-Joseph, *Science,* 2011, **331**, 183-185.
2 L. Espinar, M. Dies, T. Cagatay, G. M. Suel and J. Garcia-Ojalvo, *Proc. Natl. Acad. Sci. U. S. A.,* 2013, **110**, 7091-7096.
3 B. A. Lazazzera, *Curr. Opin. Microbiol.,* 2000, **3**, 177-182.
4 W. L. Ng and B. L. Bassler, *Annu. Rev. Genet.,* 2009, **43**, 197-222.
5 L. You, R. S. Cox, 3rd, R. Weiss and F. H. Arnold, *Nature,* 2004, **428**, 868-871.
6 I. B. Bischofs, J. A. Hug, A. W. Liu, D. M. Wolf and A. P. Arkin, *Proc. Natl. Acad. Sci. U. S. A.,* 2009, **106**, 6459-6464.
7 D. An, T. Danhorn, C. Fuqua and M. R. Parsek, *Proc. Natl. Acad. Sci. U. S. A.,* 2006, **103**, 3828-3833.
8 C. R. Boehm, P. S. Freemont and O. Ces, *Lab Chip,* 2013, **13**, 3426-3432.
9 M. E. Hibbing, C. Fuqua, M. R. Parsek and S. B. Peterson, *Nat. Rev. Microbiol.,* 2010, **8**, 15-25.
10 H. J. Kim, J. Q. Boedicker, J. W. Choi and R. F. Ismagilov, *Proc. Natl. Acad. Sci. U. S. A.,* 2008, **105**, 18188-18193.
11 D. M. Cornforth and K. R. Foster, *Nat. Rev. Microbiol.,* 2013, **11**, 285-293.
12 M. J. Kirisits, J. J. Margolis, B. L. Purevdorj-Gage, B. Vaughan, D. L. Chopp, P. Stoodley and M. R. Parsek, *J. Bacteriol.,* 2007, **189**, 8357-8360.
13 S. P. Diggle, A. S. Griffin, G. S. Campbell and S. A. West, *Nature,* 2007, **450**, 411-414.
14 S. E. Darch, S. A. West, K. Winzer and S. P. Diggle, *Proc. Natl. Acad. Sci. U. S. A.,* 2012, **109**, 8259-8263.
15 A. B. Theberge, E. Mayot, A. El Harrak, F. Kleinschmidt, W. T. Huck and A. D. Griffiths, *Lab Chip,* 2012, **12**, 1320-1326.
16 H. N. Joensson, M. L. Samuels, E. R. Brouzes, M. Medkova, M. Uhlen, D. R. Link and H. Andersson-Svahn, *Angew. Chem. Int. Ed.,* 2009, **48**, 2518-2521.
17 H. H. Jeong, S. H. Lee and C. S. Lee, *Biosens. Bioelectron.,* 2013, **47**, 278-284.
18 H. H. Jeong, Y. G. Kim, S. C. Jang, H. Yi and C. S. Lee, *Lab Chip,* 2012, **12**, 3290-3295.
19 K. P. Kim, Y. G. Kim, C. H. Choi, H. E. Kim, S. H. Lee, W. S. Chang and C. S. Lee, *Lab Chip,* 2010, **10**, 3296-3299.
20 R. S. Boogar, R. Gheshlaghi and M. A. Mahdavi, *Korean J. Chem. Eng.,* 2013, **30**, 45-49.
21 A. B. Theberge, F. Courtois, Y. Schaerli, M. Fischlechner, C. Abell, F. Hollfelder and W. T. Huck, *Angew. Chem. Int. Ed.,* 2010, **49**, 5846-5868.
22 R. R. Pompano, W. S. Liu, W. B. Du and R. F. Ismagilov, *Annu. Rev. Anal. Chem.,* 2011, **4**, 59-81.
23 O. J. Miller, A. El Harrak, T. Mangeat, J. C. Baret, L. Frenz, B. El Debs, E. Mayot, M. L. Samuels, E. K. Rooney, P. Dieu, M. Galvan, D. R. Link and A. D. Griffiths, *Proc. Natl. Acad. Sci. U. S. A.,* 2012, **109**, 378-383.
24 X. Z. Niu, F. Gielen, J. B. Edel and A. J. deMello, *Nat. Chem.,* 2011, **3**, 437-442.
25 M. Sun, S. S. Bithi and S. A. Vanapalli, *Lab Chip,* 2011, **11**, 3949-3952.
26 S. L. Sjostrom, Y. P. Bai, M. T. Huang, Z. H. Liu, J. Nielsen, H. N. Joensson and H. A. Svahn, *Lab Chip,* 2014, **14**, 806-813.
27 W. W. Shi, H. Wen, Y. Lu, Y. Shi, B. C. Lin and J. H. Qin, *Lab Chip,* 2010, **10**, 2855-2863.
28 S. Juul, Y. P. Ho, J. Koch, F. F. Andersen, M. Stougaard, K. W. Leong and B. R. Knudsen, *Acs Nano,* 2011, **5**, 8305-8310.
29 J. Xu, B. Ahn, H. Lee, L. F. Xu, K. Lee, R. Panchapakesan and K. W. Oh, *Lab Chip,* 2012, **12**, 725-730.
30 K. Leung, H. Zahn, T. Leaver, K. M. Konwar, N. W. Hanson, A. P. Page, C. C. Lo, P. S. Chain, S. J. Hallam and C. L. Hansen, *Proc. Natl. Acad. Sci. U. S. A.,* 2012, **109**, 7665-7670.
31 M. Sun and S. A. Vanapalli, *Anal. Chem.,* 2013, **85**, 2044-2048.
32 J. Shemesh, T. Ben Arye, J. Avesar, J. H. Kang, A. Fine, M. Super, A. Meller, D. E. Ingber and S. Levenberg, *Proc. Natl. Acad. Sci. U. S. A.,* 2014, **111**, 11293-11298.
33 S. L. Sjostrom, H. N. Joensson and H. A. Svahn, *Lab Chip,* 2013, **13**, 1754-1761.
34 A. R. Abate, T. Hung, P. Mary, J. J. Agresti and D. A. Weitz, *Proc. Natl. Acad. Sci. U. S. A.,* 2010, **107**, 19163-19166.
35 M. Sun, Z. S. Khan and S. A. Vanapalli, *Lab Chip,* 2012, **12**, 5225-5230.
36 S. S. Bithi, W. S. Wang, M. Sun, J. Blawzdziewicz and S. A. Vanapalli, *Biomicrofluidics,* 2014, **8**, 034118.
37 W. S. Choi, D. Ha, S. Park and T. Kim, *Biomaterials,* 2011, **32**, 2500-2507.
38 T. Yaguchi, S. Lee, W. S. Choi, D. Kim, T. Kim, R. J. Mitchell and S. Takayama, *Analyst,* 2010, **135**, 2848-2852.
39 R. Ravi, L. Philip and T. Swaminathan, *Korean J. Chem. Eng.,* 2013, **30**, 1770-1774.
40 B. Y. Jeon, J. Y. Yi and D. H. Park, *Korean J. Chem. Eng.,* 2014, **31**, 475-484.
41 H. Boukellal, S. Selimovic, Y. Jia, G. Cristobal and S. Fraden, *Lab Chip,* 2009, **9**, 331-338.
42 W. H. Tan and S. Takeuchi, *Proc. Natl. Acad. Sci. U. S. A.,* 2007, **104**, 1146-1151.
43 E. Brouzes, A. Carniol, T. Bakowski and H. H. Strey, *RSC Adv.,* 2014, **4**, 38542-38550.
44 F. K. Balagadde, L. You, C. L. Hansen, F. H. Arnold and S. R. Quake, *Science,* 2005, **309**, 137-140.
45 S. H. Hong, M. Hegde, J. Kim, X. Wang, A. Jayaraman and T. K. Wood, *Nat. Commun.,* 2012, **3**, 613.
46 S. K. Hansen, P. B. Rainey, J. A. Haagensen and S. Molin, *Nature,* 2007, **445**, 533-536.
47 M. E. Lidstrom and M. C. Konopka, *Nat. Chem. Biol.,* 2010, **6**, 705-712.
48 B. Meier, A. Zielinski, C. Weber, D. Arcizet, S. Youssef, T. Franosch, J. O. Radler and D. Heinrich, *Proc. Natl. Acad. Sci. U. S. A.,* 2011, **108**, 11417-11422.
49 R. Stocker, *Science,* 2012, **338**, 628-633.
50 S. Kim, H. J. Kim and N. L. Jeon, *Integr. Biol.,* 2010, **2**, 584-603.
51 M. S. Mauter, A. Fait, M. Elimelech and M. Herzberg, *Environ. Sci. Technol.,* 2013, **47**, 6223-6230.
52 J. Wu, Q. Chen, W. Liu and J. M. Lin, *Lab Chip,* 2013, **13**, 1948-1954.
53 W. Liu, Y. Zhang, S. Thomopoulos and Y. Xia, *Angew. Chem. Int. Ed.,* 2013, **52**, 429-432.
54 S. N. Bhatia, U. J. Balis, M. L. Yarmush and M. Toner, *FASEB J.,* 1999, **13**, 1883-1900.
55 L. Liu, B. D. Ratner, E. H. Sage and S. Jiang, *Langmuir,* 2007, **23**, 11168-11173.
56 F. R. Blattner, G. Plunkett, C. A. Bloch, N. T. Perna, V. Burland, M. Riley, J. ColladoVides, J. D. Glasner, C. K. Rode, G. F. Mayhew, J. Gregor,

N. W. Davis, H. A. Kirkpatrick, M. A. Goeden, D. J. Rose, B. Mau and Y. Shao, *Science,* 1997, **277**, 1453-1462.
57 H. Youk and W. A. Lim, *Science,* 2014, **343**, 1242782.
58 T. Defoirdt, N. Boon and P. Bossier, *PLoS Pathog.,* 2010, **6**, e1000989.
59 S. De Monte, F. d'Ovidio, S. Dano and P. G. Sorensen, *Proc. Natl. Acad. Sci. U. S. A.,* 2007, **104**, 18377-18381.

